Probabilistic Dynamic Crowd Prediction for Social Navigation

Stefan H. Kiss[1], Kavindie Katuwandeniya[1], Alen Alempijevic[1], and Teresa Vidal-Calleja[1]

Abstract— In this paper, we present a novel approach that predicts spatially and temporally crowd behaviour for robotic social navigation. Integrating mobile robots into human society involves the fundamental problem of navigation in crowds. A robot should attempt to navigate in a way that is minimally invasive to the humans in its environment. However, planning in a dynamic environment is difficult as the environment must be predicted into the future. This problem has been thoroughly studied considering the behaviour of pedestrians at the level of individuals. Instead, we represent a pedestrian crowd by its macroscopic properties over space, such as density and velocity. With this spatial representation, we propose to learn a convolutional recurrent model to predict these properties into the future. The key design of a probabilistic loss function capturing the crowd's macroscopic properties empowers the spatio-temporal crowd prediction. Using a social invasiveness metric defined on these properties predicted by our convolutional recurrent model, we develop a framework that produces globally-optimal plans in expectation. Extensive results using a realistic pedestrian simulator show the validity and performance of the proposed social navigation approach.

I. Introduction

We live in a world where robots and humans co-exist; understanding each other's intention and behaviour is crucial for safe interactions. When navigating in a dynamic crowd, humans tend to anticipate the motion of other nearby agents and plan accordingly to reach a destination. This behaviour anticipation allows the humans to manoeuvre in crowds with minimum social invasiveness. Thus, humans comply to social norms when traversing pedestrian crowds.

Robots have been deployed in crowded environments ever since late 1990s at the Deutsches Museum in Bonn, Germany [1]. They are used in airports [2], museums [3], downtown side walks [4], shopping malls [5] and numerous other populated environments. However, socially compliant robot navigation is a difficult problem.

Robot motion planning in dynamic environments is a large and active research area, covering a wide variety of approaches, from potential field [6], velocity obstacle [7], and graph-based [8] methods to reinforcement learning [9]. In developing planners for dynamic crowds, different work has focused on different goals such as reaching the destination as efficiently as possible [1], [10], or maneuvering through a crowd with as much human-like motion as possible [9]. Our objective is to develop a planner which reaches the destination minimising *social invasiveness*.

In all of these scenarios, the robot's goal is to reach a destination, while manoeuvring through a changing environment. Many approaches can be described as a form of model predictive control; utilising a receding horizon prediction and
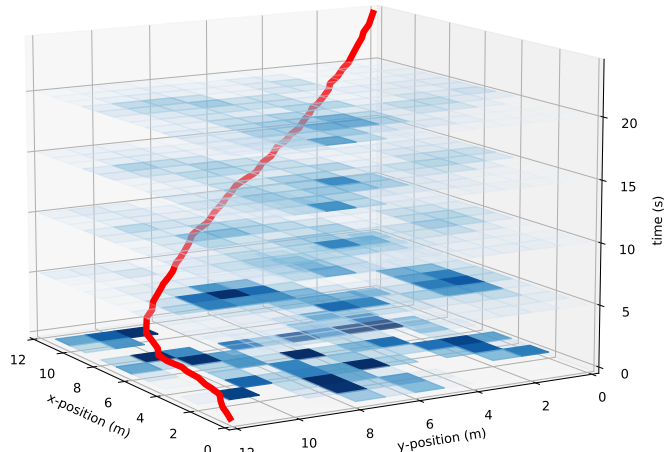

Fig. 1. A minimally invasive trajectory planned through a dynamic pedestrian crowd. The predicted crowd density through time is shown in 5 semitransparent slices. The blue cell colour represents the crowd density, darker being more dense. Note time increases from bottom to top.

optimising over a short window. Such approaches require the existence of the titular "predictive model".

Crowd-modelling has been studied in the past with various objectives [11]: crowd planning, management and evacuation [12]; entertainment (movies and games) [13]; and traffic flow [14]. It is a complex problem since the crowd can impact an individual, and an individual can impact the whole crowd.

Crowds can be modelled based on their microscopic or macroscopic properties. Microscopic modelling focuses on the behaviour of individual pedestrians and their interactions with others, while macroscopic modelling techniques focus on the crowd behaviour as a whole. While microscopic modelling is more applicable to sparse crowds with small numbers of pedestrians and few interactions, macroscopic modelling is more suitable when crowd densities are high and the total number of pedestrians modelled is large.

Crowd prediction using microscopic properties are often based on Helbing's seminal work on *social forces* [15], [16], [17], and metrics inspired by social forces such as interaction feature strings [18]. The main issue with many of these methods is that they are specifically hand-engineered to model the crowd.

Data driven approaches have advanced over the last few decades, providing an alternative to hand-engineering specific rules. In the space of data driven approaches, crowds have been modelled by their microscopic properties such as relative distance between agents in a scene [19]; hidden state sharing of nearby agents in a Recurrent Neural Network (RNN) [20]; or Euclidean distance between

[1]With the University of Technology Sydney, NSW Australia.

agents, bearing angle of agents, and distance of closest approach [21].

Analyzing crowds using gas-kinetic and fluid-dynamic models can be first found in [22] and [23]. Later, [24] modelled the crowd as a continuum fluid with a density and flow velocity, while [25] modelled crowd interactions via a dynamic potential field. In our previous work [26], we modelled the crowd based on its stationary (constant in time) macroscopic properties.

One of the major reasons for modelling crowds using microscopic crowd behaviour is that people tend to have distinct characteristics and personal goals [25]. However, when doing so, each individual has to be tracked and predicted separately. Moreover, computation time grows with the number of pedestrians in a scene. Microscopic properties, describing individuals, have less freedom at higher crowd densities [24] and thus have a low effect on the overall crowd behaviour. This emphasizes the importance of using macroscopic properties at larger scales.

Thus, we propose a framework using macroscopic crowd properties to probabilistically model the behaviour of the crowd into an uncertain future, and subsequently use the predictions to plan a trajectory through the crowd minimising the expected social invasiveness, shown in Fig. 1. This work extends our previous work [26] from a stationary flow field to the dynamic flow case, allowing current and ongoing observations to inform and improve the robot's trajectory.

We also note that our approach does not suffer from the *freezing robot problem* [27] that occurs with receding horizon methods. As our predictions effectively capture the future uncertainty, we are able to plan minimising the expected invasiveness all the way to the destination. Since the near-future is more certain, actions in the present are deemed less costly and actively encouraged.

II. BACKGROUND

A. Continuous Crowd Representation

As per our previous work [26], let us describe the crowd by a set of macroscopic properties defined as continuous functions over the underlying space. The *density* function $\rho(\mathbf{x})$ is defined as the expected number of pedestrians at position $\mathbf{x}$, per unit area. This describes how crowded different parts of the environment are. The mean *velocity* function $\boldsymbol{\mu}_{\mathbf{v}}(\mathbf{x})$ is defined as the expected velocity of pedestrians found at position $\mathbf{x}$. This describes the predominant flow of the crowd. Finally, the velocity *variance* function $\sigma_{\mathbf{v}}^2(\mathbf{x})$ represents the scalar variance of the velocity of pedestrians found at position $\mathbf{x}$. This describes the variability or irregularity of the crowd flow. A visualisation of the crowd representation is given in Fig. 2.

We assume that such properties can be captured for the entire environment of interest, such as from an overhead perspective. However, this is not a troublesome constraint as many crowded pedestrian spaces of interest (such as train stations, airports, shopping centres, and popular courtyards) have high ceilings or other elevated structures amenable to such sensing modalities.
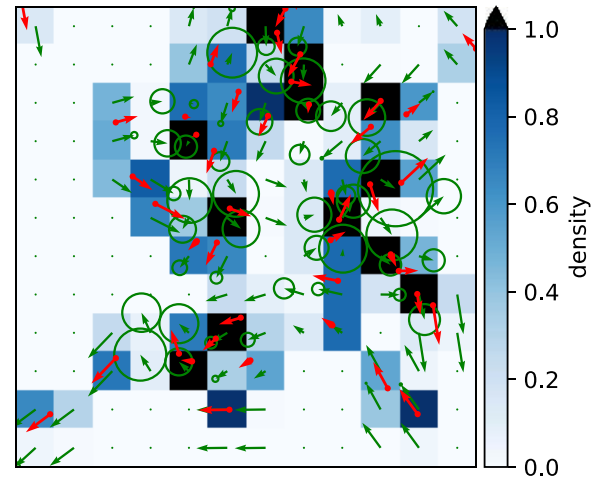

Fig. 2. A pedestrian crowd, and its macroscopic properties. The red points and arrows represent pedestrians at one instance in time. The continuous crowd representation is shown underneath, on a discretised grid generated using the method outlined in Section VI. The blue cell colour represents the density ρ. The green arrows represent the mean velocities $\boldsymbol{\mu}_{\mathbf{v}}$. The green circles, centered at the head of each arrow, represent the velocity variances, with radii of one standard deviation $\sigma_{\mathbf{v}}$.

B. Social Invasiveness Metric

A robot's presence, at position $\mathbf{x}_r$ with velocity $\mathbf{v}_r$, will interfere with the crowd. The social invasiveness metric is derived, crucially depending only on the macroscopic properties of the crowd representation, as

$$\mathcal{I}_r = \rho(\mathbf{x}_r)\left(\|\boldsymbol{\mu}_{\mathbf{v}}(\mathbf{x}_r) - \mathbf{v}_r\|^2 + \sigma_{\mathbf{v}}^2(\mathbf{x}_r)\right). \quad (1)$$

This definition of $\mathcal{I}_r$ captures a *rate* of invasiveness; to calculate the *total* invasiveness of a trajectory, this value needs to be integrated over time as in (3).

This definition of invasiveness is proportional to two factors: the expected number of interactions the robot will have with the crowd, and the magnitude of the relative velocity (and thus inversely proportional to the available time to act). More detail on the derivation of the crowd representation and the associated social invasiveness metric can be found in our previous work [26].

Note that $\mathcal{I}_r$ can be rigorously interpreted as an expectation, given the probabilistic nature of the macroscopic representation, a feature we exploit in Section IV.

C. Spatio-Temporal Prediction

Spatio-temporal learning is a non-trivial problem due to the dimensionality of the space. It requires learning both the spatial correlations and their sequential nature to be able to forecast (by definition: extrapolate) into the future.

A framework for spatio-temporal prediction was presented in [29] to approach the difficult problem of precipitation forecasting. A model is learnt to predict future radar echo maps from previous observations. The approach employs an encoder-forecaster structure consisting of ConvRNN blocks. The encoder-forecaster structure was later improved in [28].
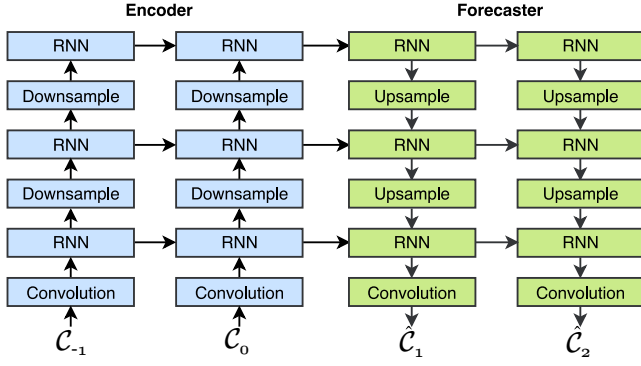
Fig. 3. The ConvRNN encoder-forecaster model. Observations from the past $\mathcal{C}_{-1}$ and $\mathcal{C}_0$ are used to generate predictions into the future $\hat{\mathcal{C}}_1$ and $\hat{\mathcal{C}}_2$. This structure can be repeated for arbitrary input and output sequence lengths. Figure adapted from [28].

The approach tackles each of the issues of spatio-temporal prediction in turn. The *spatial* relationships between features are captured by Convolutional Neural Network (CNN) blocks. Sets of 2-dimensional kernels are applied to the input images. As is common for convolutional frameworks, higher-level features are captured by downsampling layers, with successively lower spatial resolutions. The *temporal* relationships are captured by Recurrent Neural Network (RNN) blocks. In addition to mapping input to output (vertically), RNN blocks also pass hidden states sequentially through time (horizontally, see Fig. 3). To capture the spatial and temporal correlations together, the linear operations of a traditional RNN block are replaced with convolutional operations; producing a ConvRNN block.

A tower of ConvRNN and downsampling blocks is iterated temporally for each input observation, encoding a sequence of input images to a set of hidden feature images at multiple resolutions. A similar tower, reversed with upsampling replacing downsampling, transforms the encoded images into output predictions at future time steps. The recurrent nature of the encoder-forecaster framework lends itself particularly well to online usage, as hidden states can be stored, rendering each observation integration or prediction a constant-time operation.

We use this architecture as a basis to tackle the problem of forecasting dynamic pedestrian crowds.

III. PROBLEM FORMULATION

The robot is modeled as a point $\mathbf{x}_r$ in a 2-dimensional space $\mathbb{X} \subset \mathbb{R}^2$ with velocity $\mathbf{v}_r \in \mathbb{R}^2$. The robot's trajectory, defining both position and velocity through time, is given by ψ_r in the space of all continuous trajectories $\Psi \in \mathbb{R} \to \mathbb{X}$:

$$
\begin{aligned}
\mathbf{x}_r &= \psi_r(t)\,, \\
\mathbf{v}_r &= \dot{\psi}_r(t)\,.
\end{aligned}
\tag{2}
$$

A pedestrian crowd $\mathcal{C}$ exists in the environment, changing over space and time, described by its macroscopic properties *density* ρ, mean *velocity* $\boldsymbol{\mu}_{\mathbf{v}}$, and velocity *variance* $\sigma_{\mathbf{v}}^2$ (described in Section II-A). The expected *social invasiveness* of the robot $\mathcal{I}_r$, as formulated in Section II-B, is defined in

terms of these properties, locally at the position and time of the robot's presence.

At time t, the robot can observe the crowd properties $\mathcal{C}_t$.

Problem 1. *Given past observations of the crowd $\mathcal{C}_{t \leq 0}$, a measure of expected invasiveness $\mathcal{I}_r$, the robot's dynamics (2), its current position $\mathbf{x}_{curr}$, and goal position $\mathbf{x}_{goal}$; find the trajectory minimising the total expected invasiveness:*

$$
\psi_r^*, T^* = \underset{\substack{\psi_r \in \Psi \\ T \in \mathbb{R}_{\geq 0}}}{\arg\min} \int_0^T \mathbb{E}\left[\mathcal{I}_r \mid \mathcal{C}_{t \leq 0}\right] \mathrm{d}t
\tag{3}
$$

where

$$
\begin{aligned}
\psi_r(0) &= \mathbf{x}_{curr}\,, \text{ and} \\
\psi_r(T) &= \mathbf{x}_{goal}\,.
\end{aligned}
$$

We note that this formulation informs the robot only of the macroscopic properties of the crowd. As such, to avoid collision with individual pedestrians, lower-level sensing and collision avoidance behaviours would need to be incorporated into any real-world system; this is not considered further in this paper.

To approach this problem, we first construct a model to predict the crowd properties into the future. Subsequently, the optimal trajectory is found using a sampling-based motion planning algorithm.

IV. PROBABILISTIC CROWD PREDICTION

A. Probabilistic Crowd Representation

Let us emphasise the probabilistic interpretation of the crowd representation using the properties describe in Section II-A. These macroscopic properties describe statistical moments of a *Marked Spatial Point Process*. A realisation of this random process $\mathcal{C}$ is a set of positions $\mathbf{x}_i$ (representing pedestrian locations), each *marked* with an associated velocity $\mathbf{v}_i$:

$$
(\mathbf{x}_i, \mathbf{v}_i) \in \mathcal{C}\,.
\tag{4}
$$

The crowd *density* $\rho(\mathbf{x})$ is the *intensity function* of the spatial point process:

$$
\mathbb{E}\left[N_{\mathcal{C}}(B)\right] = \iint_{\mathbf{x} \in B} \rho(\mathbf{x})\, \mathrm{d}\mathbf{x}^2\,,
\tag{5}
$$

where $N_{\mathcal{C}}$ is the counting process of the point process. Intuitively, the expected number of pedestrians within region B is given by the total density within that region.

The spatial point process is *marked* by the addition of pedestrian velocities. The first and second moments of the velocity distribution are described as

$$
\begin{aligned}
\boldsymbol{\mu}_{\mathbf{v}}(\mathbf{x}) &= \mathbb{E}\left[\mathbf{v}_i \mid \mathbf{x}_i = \mathbf{x}\right] \\
\sigma_{\mathbf{v}}^2(\mathbf{x}) &= \mathrm{Var}\left[\mathbf{v}_i \mid \mathbf{x}_i = \mathbf{x}\right]\,,
\end{aligned}
\tag{6}
$$

where $\mathrm{Var}\left[\cdot\right]$ indicates the *scalar* variance, defined as the expected value of the squared Euclidean distance from the mean: $\mathrm{Var}\left[\mathbf{x}\right] = \mathbb{E}\left[\|\mathbf{x} - \mathbb{E}\left[\mathbf{x}\right]\|^2\right]$. Note that just as the intensity function of the point process can vary over space, so too can the velocity distribution.

In practice, the crowd representation is discretised over space and time, which could conceivably be captured as a video stream from an overhead camera. Thus, the crowd properties ρ, $\boldsymbol{\mu_v}$, and σ_v^2 are approximated as piece-wise constant with respect to $\mathbf{x}$ and t.

B. Learning Crowd Prediction

Based on the ConvGRU model proposed in [28] and described in Section II-C, we propose a variant where the input is a sequence of n observations of the crowd properties $\mathcal{C}_{1-n:0}$, and learn a model f_θ to estimate h future observations $\hat{\mathcal{C}}_{1:h}$:

$$\hat{\mathcal{C}}_{1:h} = f_\theta\left(\mathcal{C}_{1-n:0}\right) . \tag{7}$$

The input observations: raster images over space of $\left[\rho, \boldsymbol{\mu_v}, \sigma_v^2\right]$ (with a channel dimension size of four: 1 for ρ, 2 for vector $\boldsymbol{\mu_v}$, and 1 for scalar σ_v^2), are fed sequentially into the encoding tower. The forecasting tower produces a corresponding sequence of predictions, as raster images like the input. The density ρ and velocity variance σ_v^2 channels are exponentiated (element-wise) to constrain their values positive.

As our predicted quantities represent moments of the random variables of the crowd, we can optimise the proposed model parameters by Maximum Likelihood Estimation (MLE) if we assume the underlying distributions. Note that this is largely different from [28], where the loss function is simply deterministic.

Now let us assume the crowd point process is Poisson, thus the number of pedestrians found in any region is a Poisson random variable, independent of neighbouring regions:

$$N_{\mathcal{C}}(B) \sim \text{Poisson}\left(\iint_{\mathbf{x}\in B} \rho(\mathbf{x})\,\mathrm{d}\mathbf{x}^2\right) . \tag{8}$$

We also assume $\boldsymbol{\mu_v}(\mathbf{x})$ and $\sigma_v^2(\mathbf{x})$ describe a 2-dimensional isotropic Normal distribution,

$$\mathbf{v}_i \sim \mathcal{N}\left(\boldsymbol{\mu_v}(\mathbf{x}_i), \sigma_v^2(\mathbf{x}_i)\mathbb{I}_2\right) . \tag{9}$$

Then the MLE is formulated by minimising the cross entropy of the predicted distributions with respect to the true data. This is equivalent to minimising the forward Kullback-Leibler (KL) divergence.

The parameters θ of the model (7) are optimized by

$$\theta^* = \arg\min_\theta \sum_{\tau=1}^h D_{KL}\left(\mathcal{C}_\tau \middle\| \hat{\mathcal{C}}_\tau\right) , \tag{10}$$

where h is the prediction horizon used during training.

Taking the KL divergence between point processes is computed by applying Campbell's theorem. The nature of the marked point process requires the velocity terms to be weighted by the intensity ρ;

$$D_{KL}\left(\mathcal{C}\middle\|\hat{\mathcal{C}}\right) = \iint_{\mathbf{x}\in\mathbb{X}} D_{KL}(\text{Poisson}\,(\rho)\|\text{Poisson}\,(\hat{\rho}))$$
$$+ \rho\,D_{KL}\left(\mathcal{N}\left(\boldsymbol{\mu_v}, \sigma_v^2\mathbb{I}_2\right)\middle\|\mathcal{N}\left(\hat{\boldsymbol{\mu}}_v, \hat{\sigma}_v^2\mathbb{I}_2\right)\right)\mathrm{d}\mathbf{x}^2 . \tag{11}$$

Note that ρ, $\boldsymbol{\mu_v}$, σ_v^2, and their estimations all depend on position $\mathbf{x}$, however this dependence is elided for notational brevity.

The KL divergence between respectively Poisson random variables and 2-dimensional isotropic normal variables are:

$$D_{KL}(\text{Poisson}\,(\rho)\|\text{Poisson}\,(\hat{\rho}))$$
$$= \rho\log\frac{\rho}{\hat{\rho}} + \hat{\rho} - \rho , \tag{12}$$

$$D_{KL}\left(\mathcal{N}\left(\boldsymbol{\mu_v}, \sigma_v^2\mathbb{I}_2\right)\middle\|\mathcal{N}\left(\hat{\boldsymbol{\mu}}_v, \hat{\sigma}_v^2\mathbb{I}_2\right)\right)$$
$$= \frac{1}{2\hat{\sigma}_v^2}\|\hat{\boldsymbol{\mu}}_v - \boldsymbol{\mu_v}\|^2 + \frac{\sigma_v^2}{\hat{\sigma}_v^2} - \log\frac{\sigma_v^2}{\hat{\sigma}_v^2} - 1 . \tag{13}$$

We note that many of these terms can be ignored for the purposes of minimisation as only the estimated properties $\hat{\mathcal{C}}$ depend on the model parameters θ.

V. PLANNING AND RE-PLANNING

Once the environment can be estimated into the future, so too can the associated cost of prospective trajectories into that future. Using the asymptotically-optimal Probabilistic RoadMap (PRM*) algorithm, we randomly sample states in position and time, and connect neighbours forwards in time to form a graph.

While we do not explicitly consider the existence of any static obstacles, we note that their inclusion into both the prediction and planning phases of the framework would be trivial.

Starting from the robot's initial position, the graph is explored using Dijkstra's algorithm. Edge costs are evaluated when reached, as per the invasiveness definition (1). The associated integration is performed along a straight line path at a constant velocity; values for density ρ, velocity mean $\boldsymbol{\mu_v}$ and variance σ_v^2 are obtained by ray-tracing through the raster prediction volume.

Through prediction and planning, the crowd influences the path of the robot; however the influence of the robot's path on the crowd prediction is neglected. As the aim of the optimisation in (3) is to minimise this interaction, we assume this influence to be small (from the macroscopic perspective) and can safely ignore it.

VI. EXPERIMENTS

The predictive model and planning framework is evaluated on a simulated dataset. The well known "`pedsim`" pedestrian simulator [2] was used to generate a dense crowd scenario. This point-based data was rasterised to gridded volumetric data, with spatial resolution $1\mathrm{m}\times1\mathrm{m}$ and temporal resolution $0.5\mathrm{s}$. A Hann filter was applied to the spatial dimension to smooth the result. Positions and velocities were accumulated over time to generate the required moments: density ρ, mean velocity $\boldsymbol{\mu_v}$, and velocity variance σ_v^2 as in Fig. 2.

We consider this rasterisation process generates a dataset similar to one that could conceivably be generated from a system with an overhead video camera, without tracking individual pedestrians.
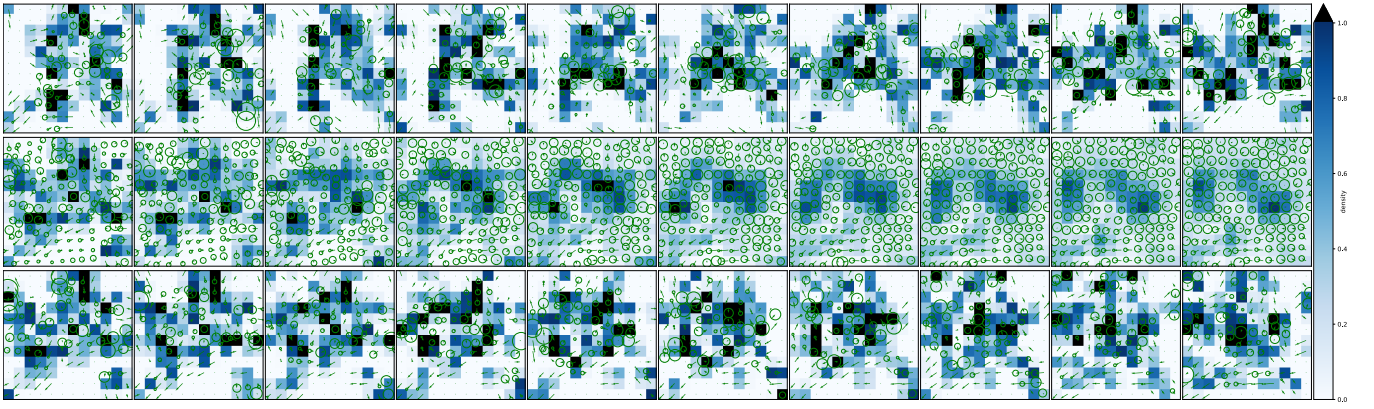
Fig. 4. Macroscopic crowd prediction. From top to bottom: a time sequence of 10 observations **input** into the model $\mathcal{C}_{-9:0}$, the 10 successive **predictions** $\hat{\mathcal{C}}_{1:10}$, and the 10 respective **ground-truth** values $\mathcal{C}_{1:10}$.
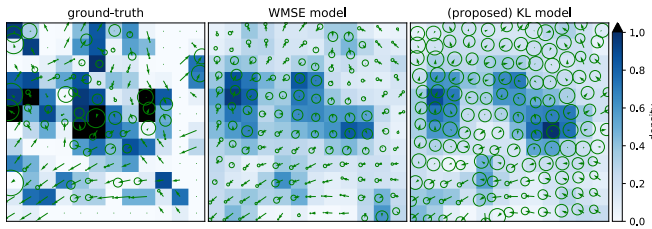

Fig. 5. Qualitative comparison of predictions between different model optimisation functions. Two models are informed with 10 observations and used to predict 10 frames into the future ($n = 10, h = 10$). The crowd properties are shown as described in the caption of Fig. 2. From left to right: the true crowd properties $\mathcal{C}_{10}$, the the predicted crowd properties $\hat{\mathcal{C}}_{10}$ from the MSE model, and the the predicted crowd properties $\hat{\mathcal{C}}_{10}$ from the proposed KL model.

A. Prediction Results

The model (7) for crowd behaviour prediction was designed and optimized as described in Section IV-B. An example of the models' output is given in Fig. 4. The model was trained on input and output sequence lengths (n and h respectively) of 10 frames (5s), on grids of 12×12 (12m $\times$ 12m).

It can be clearly seen that the model becomes less confident in it's predictions over time: the predicted densities become blurred over space and the velocity variances become larger while the means reduce.

In Fig. 5, we qualitatively compare the predictions of the proposed model against a similar model trained using the deterministic Weighted Mean Square Error (WMSE) loss. The WMSE model has the error in the velocity prediction weighted by the (true) density. In this way, the model is not penalised for its predicted velocity if there are no pedestrians.

It can be seen that the density predictions $\hat{\rho}$ are blurry, indicating that both models are uncertain about the exact location of pedestrians. Likewise, the predicted mean velocities $\hat{\boldsymbol{\mu}}_{\mathbf{v}}$ are quite similar. However, the predicted velocity variances $\hat{\sigma}_{\mathbf{v}}^2$ between these models are significantly different: the WMSE model is very confident in its velocity predictions whereas the KL model is quite uncertain. Comparing these predictions to the ground-truth values, it can be seen

that the WMSE model's confidence is unwarranted. Only the proposed model, trained using forward KL divergence, is able to capture the uncertainty of future predictions.

B. Planning Results

Based on the prediction from the model, the planner is developed as described in Section V.

We analysed our framework by comparing the trajectories produced by planning with four predictive crowd models:

Stationary flow: The crowd properties are approximated as constant in time, calculated from the statistical moments of a large historical dataset of crowd observations. This is equivalent to the method proposed in [26].

Proposed, once: Given $n = 10$ past crowd observations, future crowd properties are estimated using the model trained in Section VI-A. The plan is performed to completion, ignoring any further observations of the crowd.

Proposed, online: Given $n = 10$ past crowd observations, future crowd properties are estimated using the model trained in Section VI-A. As the plan is being executed, new crowd observations are acquired and are used to inform the model. At every observation (0.5s), a new plan is generated optimising with respect to the updated crowd predictions.

Omniscient: Instead of predictions, the true values of the future crowd properties are used for planning. This model is use for comparison, as the *perfect* solution.

Four different test scenarios were executed with each of predictive models and the average results compared in

TABLE I

COMPARISON OF PLANNING METHODS. LOWER COST IS BETTER.

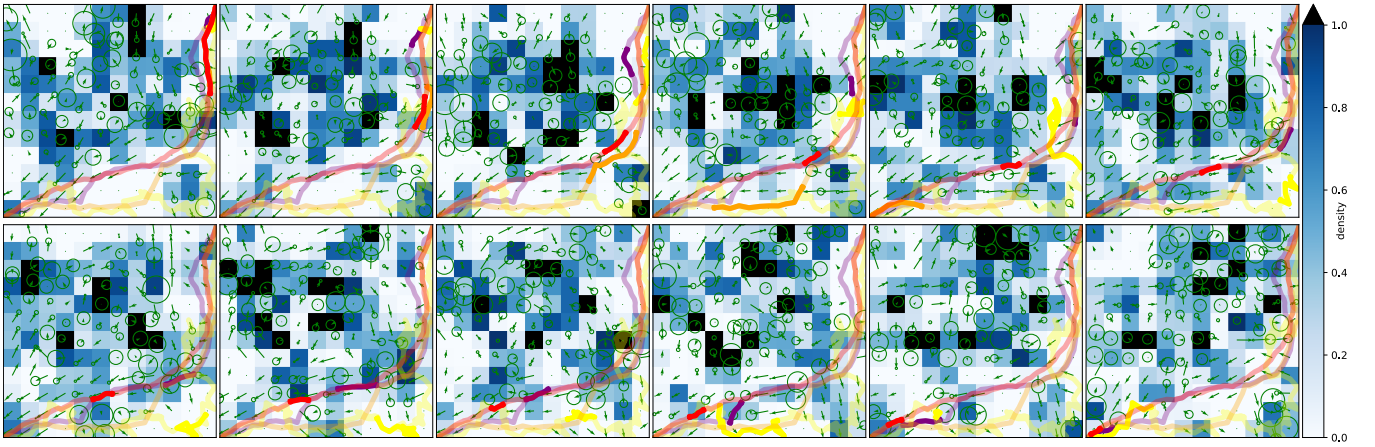| planning method	trajectory cost	
	expected	actual
stationary flow [26]	4.061	3.784
proposed, once	2.147	3.344
proposed, online	1.140	**1.124**
omniscient		0.310

Fig. 6. Planned trajectories through a dynamic crowd environment. Sequentially from left to right, then top to bottom, each frame represents 1 second in time. The crowd properties are shown as described in the caption of Fig. 2. Four trajectories, from the top-right to the bottom-left, are shown optimising the expected social invasiveness with differing crowd models: a *stationary flow* model in purple, the proposed model (run *once*) in red, the proposed model run *online* in orange, and an *omniscient* model in yellow. The full trajectories are drawn in every frame semitransparently, while the path segment traversed in the current frame is drawn opaque. See Section VI-B for details. Figure best viewed in colour.

Table I. Trajectories generated for one such scenario are shown in Fig. 6.

It can be seen that the proposed planners perform better than the stationary flow model. We note that the stationary flow model is informed in a different way to our proposed methods: the proposed models require only a short horizon of past observations $\mathcal{C}_{1-n:0}$, whereas the stationary flow model is calculated from a large historical dataset from the specific environment $\mathcal{C}_{1-M:0}$ (where $M \gg n$). This allows the stationary flow model to perform well in the repetitive simulation environment, however we doubt these results reflect the potential real-world performance under more variable conditions.

The proposed *online* framework drastically out-performs the other methods. This can be attributed to the fact that up-to-date observations of the crowd are very important for correct predictions. Over our test scenarios, this approach resulted in a 70% reduction in cost over the stationary flow assumption of [26]. Interestingly, the online planner also completed its trajectories in half the time (50% on average) compared to the other models. This can be explained by the fact that the online model can be more certain about it's immediate predictions. Comparatively, the *once* planner is uncertain about the distant future, and appropriately travels at a more conservative velocity.

The *omniscient* planner, expectedly, performs very well. We note, however, that the generated trajectory does not appear very socially-compliant. It waits and then darts between open spaces narrowly avoiding pedestrians, such behaviour would probably be quite worrying for the pedestrians involved. The proposed framework avoids this issue because the predictive model is never completely certain about existence of pedestrians or their velocities.

The solutions generated by the proposed methods minimise the expected social invasiveness, and give complete trajectories to the goal. As shown in Fig. 4, crowd predictions become more conservative into the future, which (due to the nature of the invasiveness metric) produces an incentive for the robot to reach the goal sooner. This property shows why our approach does not suffer from the *freezing robot problem* [27].

VII. CONCLUSION

We present a framework for planning in dynamic pedestrian crowds. The key aspect of the proposed framework is the spatio-temporal forecasting model that enables probabilistic prediction of the macroscopic properties of the crowd. A measure of invasiveness for a robot navigating in crowded environments is calculated using these macroscopic properties. The social navigation problem is formulated as a search to find the least invasive robot path in expectation, and is solved using the asymptotically-optimal PRM*. Our results show that our probabilistic forecaster is able to produce sequences of crowd behaviour, which are more suitable for planning under uncertainty than their deterministic counterparts. In summary, our approach enables a robot to plan a path through a dynamic crowd and reach its destination following a socially complaint trajectory.

In the future we are aiming to test our approach with a robot navigating a busy train station.

REFERENCES

[1] W. Burgard, A. B. Cremers, D. Fox, D. Hähnel, G. Lakemeyer, D. Schulz, W. Steiner, and S. Thrun, "The interactive museum tour-guide robot," in *Aaai/iaai*, 1998, pp. 11–18.

[2] R. Triebel, K. Arras, R. Alami, L. Beyer, S. Breuers, R. Chatila, M. Chetouani, D. Cremers, V. Evers, M. Fiore, *et al.*, "SPENCER: A Socially Aware Service Robot for Passenger Guidance and Help in Busy Airports," in *Field and service robotics*. Springer, 2016, pp. 607–622.

[3] F. Faber, M. Bennewitz, C. Eppner, A. Gorog, C. Gonsior, D. Joho, M. Schreiber, and S. Behnke, "The humanoid museum tour guide robotinho," in *IEEE International Symposium on Robot and Human Interactive Communication*, 2009, pp. 891–896.

[4] G. Lidoris, F. Rohrmuller, D. Wollherr, and M. Buss, "The autonomous city explorer (ace) project — mobile robot navigation in highly populated urban environments," in *2009 IEEE International Conference on Robotics and Automation*, 2009, pp. 1416–1422.

[5] A. M. Sabelli and T. Kanda, "Robovie as a mascot: a qualitative study for long-term presence of robots in a shopping mall," *International Journal of Social Robotics*, vol. 8, no. 2, pp. 211–221, 2016.

[6] S. S. Ge and Y. J. Cui, "Dynamic Motion Planning for Mobile Robots Using Potential Field Method," *Autonomous robots*, vol. 13, no. 3, pp. 207–222, 2002.

[7] P. Fiorini and Z. Shiller, "Motion Planning in Dynamic Environments Using Velocity Obstacles," *The International Journal of Robotics Research*, vol. 17, no. 7, pp. 760–772, 1998.

[8] J. J. H. Lee, C. Yoo, S. Anstee, and R. Fitch, "Efficient optimal planning in non-FIFO time-dependent flow fields," in *arXiv:1909.02198 [cs.RO]*, 2019, pp. 1–10.

[9] P. Henry, C. Vollmer, B. Ferris, and D. Fox, "Learning to navigate through crowded environments," *Proc. of IEEE ICRA*, pp. 981–986, 2010.

[10] E. Prassler, J. Scholz, and P. Fiorini, "A robotics wheelchair for crowded public environment," *IEEE Robotics Automation Magazine*, vol. 8, no. 1, pp. 38–45, 2001.

[11] K. Ijaz, S. Sohail, and S. Hashish, "A Survey of Latest Approaches for Crowd Simulation and Modeling using Hybrid Techniques," *UKSIM-AMSS International Conference on Modelling and Simulation*, pp. 111–116, 2015.

[12] N. Pelechano and N. I. Badler, "Modeling crowd and trained leader behavior during building evacuation," *IEEE computer graphics and applications*, vol. 26, no. 6, pp. 80–86, 2006.

[13] B. G. Silverman, M. Johns, J. Cornwell, and K. O'Brien, "Human behavior models for agents in simulators and games: part i: enabling science with pmfserv," *Presence: Teleoperators & Virtual Environments*, vol. 15, no. 2, pp. 139–162, 2006.

[14] J. Zhang, Y. Zheng, and D. Qi, "Deep spatio-temporal residual networks for citywide crowd flows prediction," *arXiv preprint arXiv:1610.00081*, 2016.

[15] D. Helbing and P. Molnár, "Social force model for pedestrian dynamics," *Physical Review E*, vol. 51, pp. 4282–4286, 1995.

[16] M. Luber, J. A. Stork, G. D. Tipaldi, and K. O. Arras, "People tracking with human motion predictions from social forces," in *Proc. of IEEE ICRA*, 2010, pp. 464–469.

[17] R. Mehran, A. Oyama, and M. Shah, "Abnormal crowd behavior detection using social force model," in *Proc. of IEEE Conference on CVPR*, 2009, pp. 935–942.

[18] L. Leal-Taixé, M. Fenzi, A. Kuznetsova, B. Rosenhahn, and S. Savarese, "Learning an image-based motion context for multiple people tracking," in *Proc. of IEEE Conference on CVPR*, 2014, pp. 3542–3549.

[19] A. Gupta, J. Johnson, L. Fei-Fei, S. Savarese, and A. Alahi, "Social GAN: Socially Acceptable Trajectories with Generative Adversarial Networks," *Proc. of IEEE Conference on CVPR*, pp. 2255–2264, 2018.

[20] A. Alahi, K. Goel, V. Ramanathan, A. Robicquet, L. Fei-Fei, and S. Savarese, "Social LSTM: human trajectory prediction in crowded spaces," in *Proc. of IEEE Conference on CVPR*, 2016, pp. 961–971.

[21] J. Amirian, J. B. Hayet, and J. Pettre, "Social ways: Learning multimodal distributions of pedestrian trajectories with GANs," *Proc. of IEEE Conference on CVPR Workshops*, vol. 2019-June, pp. 2964–2972, 2019.

[22] L. F. Henderson, "On the fluid mechanics of human crowd motion," *Transportation Research*, vol. 8, no. 6, pp. 509–515, 1974.

[23] D. Helbing, "A Fluid Dynamic Model for the Movement of Pedestrians," *Complex Systems*, vol. 6, pp. 391–415, 1998.

[24] R. Narain, A. Golas, S. Curtis, and M. C. Lin, "Aggregate Dynamics for Dense Crowd Simulation," *ACM Transactions on Graphics*, vol. 28, no. 5, pp. 1–8, 2009.

[25] A. Treuille, S. Cooper, and Z. Popović, "Continuum Crowds," *ACM SIGGRAPH 2006 Papers, SIGGRAPH '06*, pp. 1160–1168, 2006.

[26] S. H. Kiss, K. To, C. Yoo, R. Fitch, and A. Alempijevic, "Minimally invasive social navigation," in *ACRA*, 2019, pp. 1–8.

[27] P. Trautman and A. Krause, "Unfreezing the robot: Navigation in dense, interacting crowds," *IEEE/RSJ IROS*, pp. 797–803, 2010.

[28] X. Shi, Z. Gao, L. Lausen, H. Wang, D.-Y. Y. Yeung, W.-k. K. Wong, and W.-c. C. Woo, "Deep learning for precipitation nowcasting: A benchmark and a new model," in *NIPS*, vol. 2017-Decem, 2017, pp. 5617–5627.

[29] S. Xingjian, Z. Chen, H. Wang, D.-Y. Yeung, W.-K. Wong, and W.-c. Woo, "Convolutional lstm network: A machine learning approach for precipitation nowcasting," in *NIPS*, 2015, pp. 802–810.